



# Characterizing mandibular growth using three-dimensional imaging techniques and anatomic landmarks



Michael P. Kelly<sup>a,1</sup>, Houri K. Vorperian<sup>a,1,\*</sup>, Yuan Wang<sup>a,b</sup>, Katelyn K. Tillman<sup>a</sup>, Helen M. Werner<sup>a</sup>, Moo K. Chung<sup>a,b</sup>, Lindell R. Gentry<sup>c</sup>

<sup>a</sup> Vocal Tract Development Laboratory, Waisman Center, University of Wisconsin-Madison, 1500 Highland Ave., Rooms 429/427, Madison, WI 53705, USA

<sup>b</sup> Department of Biostatistics and Medical Informatics, University of Wisconsin-Madison, 1300 University Avenue, Madison, WI 53706, USA

<sup>c</sup> Department of Radiology, University of Wisconsin Hospital and Clinics, University of Wisconsin-Madison, Box 3252 Clinical Science Center, E1 336, 600 Highland Ave., Madison, WI 53792, USA

## ARTICLE INFO

### Article history:

Received 5 May 2016

Received in revised form 30 November 2016

Accepted 18 January 2017

### Keywords:

Mandible  
Development  
Measurement  
3DCT

## ABSTRACT

**Objective:** To provide quantitative data on the multi-planar growth of the mandible, this study derived accurate linear and angular mandible measurements using landmarks on three dimensional (3D) mandible models. This novel method was used to quantify 3D mandibular growth and characterize the emergence of sexual dimorphism.

**Design:** Cross-sectional and longitudinal imaging data were obtained from a retrospective computed tomography (CT) database for 51 typically developing individuals between the ages of one and nineteen years. The software Analyze was used to generate 104 3DCT mandible models. Eleven landmarks placed on the models defined six linear measurements (lateral condyle, gonion, and endomolare width, ramus and mental depth, and mandible length) and three angular measurements (gonion, gnathion, and lingual). A fourth degree polynomial fit quantified growth trends, its derivative quantified growth rates, and a composite growth model determined growth types (neural/cranial and somatic/skeletal). Sex differences were assessed in four age cohorts, each spanning five years, to determine the ontogenetic pattern producing sexual dimorphism of the adult mandible.

**Results:** Mandibular growth trends and growth rates were non-uniform. In general, structures in the horizontal plane displayed predominantly neural/cranial growth types, whereas structures in the vertical plane had somatic/skeletal growth types. Significant prepubertal sex differences in the inferior aspect of the mandible dissipated when growth in males began to outpace that of females at eight to ten years of age, but sexual dimorphism re-emerged during and after puberty.

**Conclusions:** This 3D analysis of mandibular growth provides preliminary normative developmental data for clinical assessment and craniofacial growth studies.

© 2017 Elsevier Ltd. All rights reserved.

## 1. Introduction

The mandible is a cornerstone of the craniofacial complex, extending inferiorly and anteriorly from the temporal bone of the cranium to form the inferior border of the face while maintaining important functional connections with the basicranium and the

maxilla. The only moving bone in the craniofacial complex, the mandible serves a number of important biological functions including sucking, swallowing, respiration, mastication, and vocalization (Coquerelle et al., 2011; Humphrey, 1998; Smartt, Low, & Bartlett, 2005a). In order for these functions to continue uninterrupted over the course of development, the myriad

**Abbreviations:** 2D, two-dimensional; 3D, three-dimensional; CDC, Centers for Disease Control and Prevention; CT, computed tomography; DICOM, digital imaging and communications in medicine; GE, general electric; HU, Hounsfield units; IRB, Institutional Review Board; NIH, National Institutes of Health; NIDCD, National Institute on Deafness and Other Communication Disorders; NICHD, National Institute of Child Health and Human Development; WHO, World Health Organization.

\* Corresponding author.

**E-mail addresses:** [mkelly1@wisc.edu](mailto:mkelly1@wisc.edu) (M.P. Kelly), [vorperian@waisman.wisc.edu](mailto:vorperian@waisman.wisc.edu), [hkvorper@wisc.edu](mailto:hkvorper@wisc.edu), <http://www.waisman.wisc.edu/vocal/> (H.K. Vorperian), [yuanw@stat.wisc.edu](mailto:yuanw@stat.wisc.edu) (Y. Wang), [kkassulke@waisman.wisc.edu](mailto:kkassulke@waisman.wisc.edu) (K.K. Tillman), [holden@wisc.edu](mailto:holden@wisc.edu) (H.M. Werner), [mkchung@wisc.edu](mailto:mkchung@wisc.edu) (M.K. Chung), [lgency@uwhealth.org](mailto:lgency@uwhealth.org) (L.R. Gentry).

<sup>1</sup> Co-equal first authors.

structures of the head and face must work and grow in concert with one another.

The growth of the craniofacial complex is governed by a combination of genetically predetermined factors and epigenetic factors such as mechanical forces, function, and trauma, which activate the expression of regulatory genes (Carlson, 2005). Throughout mandibular growth and development, passive translation by associated soft tissues and complex patterns of bone resorption and deposition alter the dimensions, shape and orientation of the mandible (Enlow & Harris, 1964; Moss & Rankow, 1968). In the young mandible, the gonion lies anterior to the condylar head. As the mandible develops, resorption at the anterior portion of the ramus and deposition at its posterior border gradually relocate the gonion, and the entire ramus, posteriorly such that it lies beneath the condylar head in the mature mandible. The condylar heads themselves are also relocated posteriorly over the course of development, which results in displacement at the temporomandibular joint (TMJ). These relocations, combined with deposition on the inferior border of the mandible, lead to the observed downward and forward growth of the mandible (Enlow & Harris, 1964; Enlow & Hans, 1996; Martinez-Maza, Rosas, & Nieto-Diaz, 2013; Moss & Rankow, 1968).

Sex differences in mandibular shape and dimensions have been reported in adulthood and during puberty (Coquerelle et al., 2011; Franklin, Oxnard, O'Higgins, & Dadour, 2007; Jacob & Buschang, 2014; Rosas & Bastir, 2002); however, findings on pre-pubertal sexual dimorphism are inconsistent despite consistent findings on sex differences in craniofacial dimensions at birth (Humphrey, 1998; Rosas & Bastir, 2002). Coquerelle et al. (2011) noted that the nature of mandibular dimorphism changes during the course of development; size dimorphism persists into adulthood, whereas shape dimorphism present at birth in the ramus and mental region become less evident between the ages 4 and 14 years, due to the more rapid growth in females.

While the general growth pattern of the mandible is understood, only a few studies have characterized in detail the quantitative changes in the size and shape of the developing mandible. Previous studies have primarily relied upon x-ray (Broadbent, Broadbent, & Golden, 1975; Bulygina, Mitteroecker, & Aiello, 2006), lateral cephalograms (Broadbent et al., 1975; Jacob & Buschang, 2014; Walker & Kowalski, 1972) and thin plate spline analysis (Bulygina et al., 2006; Rosas & Bastir, 2002). Studies that have utilized computed tomography (CT) scans have either used geometric morphometrics to analyze sexual dimorphism of mandibular surfaces during postnatal development (Coquerelle et al., 2011), or have focused on the sexual dimorphism of the mandible up until puberty, as opposed to the growth and development over the entire adolescence period (Krarup, Darvann, Larsen, Marsh, & Kreiborg, 2005). Although Bulygina et al. (2006) and Krarup et al. (2005) included three-dimensional analyses, limited quantitative measurements were derived from their 3D data. Quantifying the typical three-dimensional growth pattern and growth rate of the mandible would help establish a normative reference and range of variability for typical growth (Björk, 1969) and would help characterize the developmental changes in sexual dimorphism. Such knowledge would be an invaluable normative reference for the assessment and management of atypical or clinical cases; such as for orthodontic treatment planning (Gillgrass & Welbury, n.d.; Jacob & Buschang, 2014), and for optimizing mandibular surgical reconstruction of patients with developmental lesions who require mandibular lengthening or shortening procedures (Smartt et al., 2005a; Smartt, Low, & Bartlett, 2005b).

Structures in the head and neck exhibit a non-uniform growth pattern during the first two decades of life. Scammon (1930) outlined the primary postnatal growth types exhibited by the

majority of body structures (neural, general/somatic, lymphoid and genital) and noted that some structures exhibit a peculiar growth pattern that is a combination of those primary growth types. Structures with a neural growth type, such as the cranium, show a pattern of growth with an initial rapid growth rate reaching 80% of adult size by age five. Structures with a general or somatic growth type, such as the face, also grow rapidly in the first five years, but only attain 25–40% of adult size. Following this initial rapid growth period, both growth types exhibit slow and steady growth until maturity with an additional period of rapid growth during puberty for structures with somatic growth. Typically, it is during this latter growth period that sexual dimorphism becomes evident. Assessment of growth type can help elucidate the effect of functional versus structural relations on mandibular growth, and help identify periods where sexual dimorphism is likely to emerge.

This study aims to characterize, in three dimensions, the sex-specific growth of the typically developing mandible during approximately the first two decades of life, taking into account growth trend, growth rate and growth type (neural-somatic). It also aims to determine the growth patterns that give rise to the emergence of sexual dimorphism during the course of development. Given that the mandible is part of the craniofacial complex, we hypothesized that during typical growth, the mandible dimensions would have different growth types in different planes; mandibular width or length (in the horizontal plane) would have a predominantly neural growth type given its connection with the cranium at the TMJ and mandibular depth (in the vertical plane) would have more of a general or somatic growth type. Furthermore, we hypothesized that the mandible dimensions would be larger in males than in females during the course of development and that sexual dimorphism would become more apparent during and after adolescence.

## 2. Materials and methods

### 2.1. Medical imaging studies and image acquisition

The imaging studies used in the present study consisted of CT scans of typically developing individuals selected from a large retrospective database of head and neck imaging studies. This database was established to quantify the development of typical and atypical head and neck structures by the Vocal Tract Development Laboratory at the Waisman Center over a span of 15 years, with approval from the University of Wisconsin Health Sciences Institutional Review Board (IRB protocols: 1995-1006, 2003-1006, M-2007-1009 and 2011-0037). The inclusion of imaging studies coded as typically developing in this database entailed the screening of patients by the radiologist on the team with head and neck subspecialty for medical conditions that alter typical growth and development, as well as medical conditions that alter the growth of the mandible or skull base. Furthermore, the radiologist examined each imaging study to ensure the visualization of all head and neck structures of interest, and verification that the patient had a typical Class I bite (normognathic). A total of 104 CT studies (56 male, 48 female) with an age range of 1.01 (*years.months*) to 19 years, were selected for inclusion in this study. The scans were from 51 typically developing individuals (27 male, 24 female) as some of the scans represented longitudinal data from the same patient. For localized assessment of sex differences, this sample was divided into four age cohorts each spanning five years (*years.months*): Prepubertal cohort I ages birth to 4.11 (*n*=26, 16 M, 10 F), and cohort II ages 5.00 to 9.11 (*n*=22, 11 M, 11 F); pubertal cohort III ages 10.0 to 14.11 (*n*=25, 14 M, 11 F); and postpubertal cohort IV ages 15.00 to 19.11 (*n*=31, 15 M, 16 F). This four age-based grouping, used in Vorperian et al. (2011), roughly matches Fitch and Giedd's (1999) pubertal stage

grouping which was based on Tanner's (1962) standardized rating system of pubertal stages. Also, this grouping was successful in unveiling prepubertal sexual dimorphism of oral and pharyngeal portions of the vocal tract that would have otherwise been masked due to sex differences in growth rate (Vorperian et al., 2011). Special effort was directed to have as even a distribution across age and sex as possible for the entire sample, as well as within each of the four age cohorts.

During image acquisition, all the patients had been scanned in the supine position using the University of Wisconsin Hospital's head and neck imaging protocol, with the head/face placed centrally in the scanner and the neck in a neutral position. All scans were acquired with a 512 × 512 mm matrix. Scan field of view ranged from 13 × 13 to 30 × 30 cm, with most scans having either a 16 × 16 (n=32) or 18 × 18 (n=45) cm field of view. In-plane resolution/voxel size ranged from 0.27 to 0.59 mm, with an average of 0.33 mm. Slice thickness ranged from 1.3 to 5.0 mm, with the vast majority (97%; n=101) of scans having a 2.5 mm slice thickness. CT scans were obtained with a variety of models of high resolution, multi-slice General Electric (GE) CT scanners. Raw CT image data was reconstructed using several GE reconstruction algorithms that were obtained for optimal visualization of bony (Bone, BonePlus) and soft tissue (Standard, Soft) structures. For the present study the Standard (n=97) or Soft (n=7) tissue algorithms were used. Soft algorithms were chosen for cases where standard algorithms were not available. Images were initially stored on a McKesson Horizon Rad Station PACS system. They were then set anonymous using a General Electric Advantage Windows workstation and saved in the Digital Imaging and Communications in Medicine (DICOM) format using alphanumeric codes that preserved patient sex and age at time of imaging. For additional detail on the imaging database and scanning procedures, see Vorperian et al. (2009).

## 2.2. Image segmentation

The DICOM files were imported into the 3D biomedical image visualization and analysis software Analyze® 10.0 (AnalyzeDirect; Overland Park, KS). The mandible of each case was segmented from

the CT scan data using an image intensity thresholding technique based on Hounsfield units (HU) (Whyms et al., 2013). A global threshold (approximately 150–3071 HU) designed to exclude low-density objects such as air and soft tissue was applied to the image in order to visualize bony structures. The 3DCT mandible model was then extracted from the skeleton using the Trace tool in Analyze® 10.0's Volume Render module. Often, it proved difficult to segment both the mandibular condyles from the cranial base and the lower teeth from the upper teeth, due to the close proximity and similar density of these structures. In such cases, manual slice-by-slice editing of multiplanar reconstructions allowed for further refinement of the 3DCT models.

## 2.3. Mandibular landmarking and measurement

A total of 11 predetermined anatomic landmarks (Table 1) were placed on each of the 3DCT mandible models (Fig. 1) by two researchers using the Fabricate tool in Analyze®. Digital landmark placement was guided through the use of multiplanar reconstruction, including sagittal, coronal, and axial views of the original DICOM images, while using the 3DCT model to corroborate landmark placement. After placing landmarks, the (x, y, z) coordinates of each point were obtained using the Analyze® software.

Landmark coordinates were then extracted and linear distances and angular values were calculated using the following formulas:

$$Distance(pixels) = \sqrt{(x_1 - x_2)^2 + (y_1 - y_2)^2 + (z_1 - z_2)^2}$$

Angle(degrees) =  $\cos^{-1}((a \cdot b) / (||a|| ||b||))$ , where (x<sub>1</sub>, y<sub>1</sub>, z<sub>1</sub>) and (x<sub>2</sub>, y<sub>2</sub>, z<sub>2</sub>) are the coordinates of two landmarks and vectors a and b are represented by the vectors formed between the vertex of an angle and each of the two remaining landmarks. Linear variables were scaled by pixel size to acquire a measurement in millimeters (mm). As listed in Table 2, a total of six linear and three angular variables were examined for each case to quantify mandibular size and shape in three dimensions.

Measurement consistency was assessed by having two researchers place landmarks on 10% of the cases used in this

**Table 1**  
Mandibular landmarks used for making linear and angular measurements.

| Landmark # | Description   | Landmark Name (Abbreviation)   |
|------------|---|--------------------------------|
| 1          | The most superior point of left condylar head.  | Condyle Superior Left (CdSuLt) |
| 2          | The most supralateral point of left mandibular condyle.   | Condyle Lateral Left (CdLaLt)  |
| 3          | The most supralateral point of right mandibular condyle.  | Condyle Lateral Right (CdLaRt) |
| 4          | The most inferior, posterior, and lateral point on the left external angle of the mandible.   | Gonion Left (GoLt)             |
| 5          | The most inferior, posterior, and lateral point on the right external angle of the mandible.  | Gonion Right (GoRt)            |
| 6          | The most medio-posterior point on the last erupted tooth of the left side (molar 3 in adults), where the tooth meets the alveolar bone.                   | Endomolare Left (EnmLt)        |
| 7          | The most medio-posterior point on the last erupted tooth of the right side (molar 3 in adults), where the tooth meets the alveolar bone.                  | Endomolare Right (EnmRt)       |
| 8          | The most medial point on the left side of the lingual mandibular body (submandibular fossa ridge), in-line with the posterior border of the third molar.  | Sublingual Fossa-3L (SLF-3L)   |
| 9          | The most medial point on the right side of the lingual mandibular body (submandibular fossa ridge), in-line with the posterior border of the third molar. | Sublingual Fossa-3R (SLF-3R)   |
| 10         | The most inferior point on the symphysis menti.   | Gnathion (Gn)                  |
| 11         | The most superior point of the alveolar bone on the dorsal symphysis below the incisors.  | Posterior Dental Border (DbPo) |

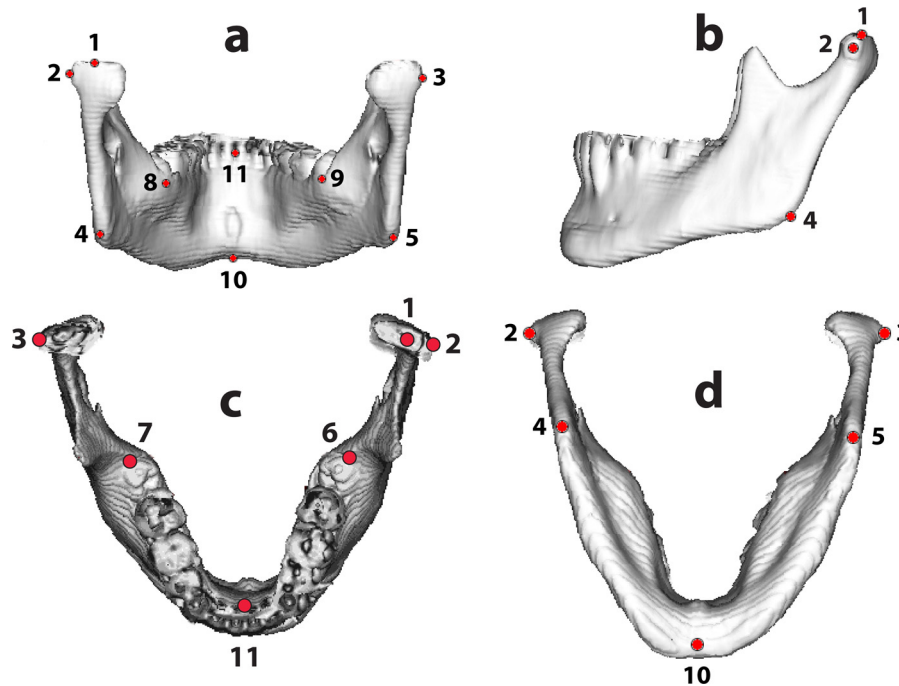


**Fig. 1.** Landmarked mandibles viewed from the (a) posterior, (b) lateral left, (c) superior, and (d) inferior perspectives. Landmarks are described in detail in Table 1, and the nine landmark-based measurements (6 linear and 3 angular measurements) are defined in Table 2.

**Table 2**

The nine mandibular variables examined. The six linear and three angular measurements are defined using the landmarks as specified in Table 1.

| Variable Name          | Landmarks used | Variable Abbreviation | Description   |
|------------------------|----------------|-----------------------|---|
| Lateral Condyle Width  | 2-3            | <i>LatCondW</i>       | The distance between the most lateral points on the left and right condylar heads of the mandible.  |
| Gonion Width           | 4-5            | <i>GonW</i>           | The distance between the left and right gonions.  |
| Endomolare Width       | 6-7            | <i>EmolW</i>          | The distance between the left and right endomolares.  |
| Mandibular Length Left | 4–10           | <i>MandL-Lt</i>       | The distance from the left gonion to the gnathion.  |
| Ramus Depth Left       | 1-4            | <i>RamD-Lt</i>        | The distance from the most superior point on the left mandibular condyle to the left gonion.  |
| Mental Depth           | 10–11          | <i>MentD</i>          | The distance between the posterior dental border and the gnathion.  |
| Gonion Angle Left      | ∠1-4–10        | <i>GonAng-Lt</i>      | The angle formed by the intersection of the lines running from the most superior point on the left mandibular condyle and the gnathion to the gonion. |
| Gnathion Angle         | ∠4–10-5        | <i>GnathAng</i>       | The angle formed by the intersection of the lines running from the left and right gonions to the gnathion.  |
| Lingual Angle          | ∠8–10-9        | <i>LingAng</i>        | The angle formed by the intersection of the lines running from <i>SLF-3L</i> and <i>SLF-3R</i> to the gnathion  |

study and measurements calculated for each of the nine variables. Next, the derived measurements were used to quantify measurement error by calculating the average relative error (ARE; Chung, Chung, Durtschi, Gentry & Vorperian, 2008). An average difference of less than 5% ( $ARE < .05$ ) between researchers is considered an acceptable standard by most studies (Whymys et al., 2013). The ARE for *LatCondW*, *GonW*, *EmolW*, *MandL-Lt*, *RamD-Lt*, *MentD*, *GonAng-Lt*, *GnathAng*, and *LingAng* was .0078, .0066, .1419, .0239, .03413, .0379, .0077, .02377 and .05239 respectively. The generally low ARE reflected consistency of landmark-based measurements among our researchers. The larger ARE for the variables endomolare width (*EmolW*) at 14.2% and lingual angle (*LingAng*) at 5.3% were likely due to difficulty with landmark placement particularly in younger cases where the molars have not erupted (landmarks 6 and 7 for *EmolW*) or the sublingual fossa is underdeveloped (landmarks 8 and 9 for *LingAng*) and require more cautious and lenient interpretation of findings particularly for endomolare width.

#### 2.4. Statistical analysis

For each variable, the male and female data was plotted as a function of age and each sex was separately fitted over the course of the age range with a fixed-effects polynomial model. Following the same analysis steps as in Vorperian et al. (2009), the fourth degree polynomial fit was determined to be optimal for our data (as compared to third or fifth degree polynomial fits). Next, data points whose externally Studentized residual exceeded 2.6 standard deviations of the t-distribution were considered outliers (as listed per age cohort in Table 3) and removed from further analyses. For variables with missing measurements, the missing data treatment entailed using the mean values of its sex-specific fixed-effects fourth order polynomial to impute the values. Next, taking into account measurement from the same subject, the sex-specific measurements for each of the nine variables were fitted with a mixed-effects fourth-degree polynomial model



(Wang, Chung, & Vorperian, 2016). Unlike the fixed-effect model, the mixed-effect model takes into account the dependency among longitudinal data from the same subject and thus provides a better fit to the data than the fixed-effect model. Finally, for all measurements the first derivative of the fixed-effects portion of the mixed-effects model was calculated to determine the sex-specific growth rates throughout the entire age range (mm/month or degrees/month for the linear and angular measurements, respectively; see Figs. 2–4, right panel).

To assess growth type, a composite growth model comprised of a linear combination of two growth types, neural and somatic, was applied to the raw data from the six linear and three angular measurements in order to determine the contribution of each type to the overall growth. As described previously (Kano et al., 2015; Vorperian et al., 2011), published normative growth curves were used to represent each of these types of growth. Neural growth was represented by head circumference data obtained from Nellhaus (1968), and somatic growth was represented by Centers for Disease Control and Prevention (CDC) height growth curves based upon several national health examination datasets taken between the years 1963 and 1994 (Fryar, Gu, & Ogden, 2012; Kuczmarski et al., 2002). As noted in the introduction, percent growth of adult size at about age 5 is an important factor when differentiating between neural and somatic growth, and therefore taken into account for all calculations and denoted by the second y-axis in Figs. 2–4. Additionally, percent growth at age 5 was calculated for all linear measurements using the polynomial fit-curve (see Table 4, last column). All measurements and calculations were sex-specific. Lastly, a two-tailed Pearson correlation was run to assess the relationship between growth at age 5 and neural contribution to growth.

Sex differences were assessed using an overall differences in male (M) versus female (F) growth trends for each of the nine variables using the likelihood ratio test. In addition, to detect localized male versus female differences in the four age-cohorts of each variable, measurements were compared by sex using a two-sample *t*-test within each of these age cohorts. To account for multiple comparisons, the Bonferroni correction (Bland & Altman, 1995) was applied at the .05 level for statistical significance.

### 3. Results

#### 3.1. Growth trends and growth rates

The growth trends for the linear variables, displayed in the left panel of Figs. 2 and 3, reveal the expected non-uniform growth trend consisting of an initial rapid growth rate during early childhood; with some variables displaying a second increase in growth rate during puberty, which was typically more pronounced for males. The only exception to this pattern was female endomolare width (*EmolW-Female*), which showed a steady growth throughout the entire period examined. Negative growth fits for linear measurements near the extreme ends of the age range (e.g., *EmolW-Male*) represent a limitation of the curve-fitting technique used.

In general, growth followed a similar trajectory for both sexes from birth to age five. The sex-specific average percent growth of the mature size for all linear variables, referenced to the right y-axes in Figs. 2 and 3 (left panel), revealed the female mandibles to be slightly closer to the adult mature size at age five (53%) than the male mandibles (49%). Individual linear measurements, however, could vary with age and sex. An extreme exception, in five-year-old males, is endomolare width (*EmolW-Male*), which reached 76% of its eventual width, while mental depth (*MentD-Male*) attained only 34% of its ultimate depth (see Table 4). The last column in Table 4 shows that in general at age five, females had larger percent growth values than males for the remaining linear variables – *LatCondW*, *GonW*, *MandL-Lt*, and *MentD*.

After age five, male mandibles tended to be of a similar or larger size than female mandibles. Around ages eight to ten years, growth in males began to outpace that in females. At fifteen to sixteen years, growth in both sexes slowed dramatically as the mandible approached its mature size. It is during this secondary growth spurt that sexual dimorphism became especially apparent, with male mandibles taking on greater dimensions than their female counterparts. The emergence of sexual dimorphism was always preceded by changes in growth rate (Figs. 2 and 3 right panel) a few years before the actual sex differences in growth trend surfaced (Figs. 2 and 3 left panel).

**Table 3**

Sex differences test result for each of the nine variables. Variable abbreviation in the first column is followed by the *p* value of the overall sex effect likelihood ratio test (in parentheses) with significant comparisons marked with an asterisk. Remaining column are the *t*-tests results examining sexual dimorphism by age Cohort (I–IV). For each *t*-test, sample size, number of outliers (discarded prior to analysis), along with test results are listed by measurement (left) and cohort (top). Bonferroni significant male/female comparisons are highlighted in bold (and marked with an asterisk).

| Variable Abbreviation ( $\chi^2$ pvalue) | Cohort I               |   | Cohort II              |   | Cohort III             |   | Cohort IV              |   |
|--|------------------------|---|------------------------|---|------------------------|---|------------------------|---|
|  | <i>n</i> (outliers)    | <i>t</i> -test results                  | <i>n</i> (outliers)    | <i>t</i> -test results                                | <i>n</i> (outliers)    | <i>t</i> -test results                                    | <i>n</i> (outliers)    | <i>t</i> -test results                                    |
| <i>LatCondW</i> ( <i>p</i> = 0.0802)     | M: 16 (1)<br>F: 10 (0) | <i>t</i> (13) = -0.01<br><i>p</i> = .99 | M: 11 (0)<br>F: 11 (0) | <i>t</i> (18) = 0.04<br><i>p</i> = .97                | M: 14 (0)<br>F: 11 (0) | <i>t</i> (17) = -1.72<br><i>p</i> = .10                   | M: 15 (0)<br>F: 16 (0) | <i>t</i> (23) = -1.67<br><i>p</i> = .11                   |
| <i>GonW</i> ( <i>p</i> = 0.0008)*        | M: 16 (1)<br>F: 10 (0) | <i>t</i> (18) = 1.15<br><i>p</i> = .27  | M: 11 (0)<br>F: 11 (0) | <i>t</i> (19) = -0.94<br><i>p</i> = .36               | M: 14 (0)<br>F: 11 (0) | <b><i>t</i>(22) = -7.06</b><br><b><i>p</i> &lt; .001*</b> | M: 15 (1)<br>F: 16 (0) | <b><i>t</i>(28) = -8.24</b><br><b><i>p</i> &lt; .001*</b> |
| <i>EmolW</i> ( <i>p</i> = 0.0466)*       | M: 16 (0)<br>F: 10 (0) | <i>t</i> (24) = 0.31<br><i>p</i> = .76  | M: 11 (0)<br>F: 11 (0) | <i>t</i> (20) = -0.07<br><i>p</i> = .95               | M: 14 (1)<br>F: 11 (0) | <i>t</i> (22) = -0.71<br><i>p</i> = .48                   | M: 15 (0)<br>F: 16 (0) | <i>t</i> (28) = -1.83<br><i>p</i> = .08                   |
| <i>MandL-Lt</i> ( <i>p</i> = 0.0414)*    | M: 16 (0)<br>F: 10 (0) | <i>t</i> (13) = 0.98<br><i>p</i> = .35  | M: 11 (0)<br>F: 11 (0) | <i>t</i> (20) = -0.62<br><i>p</i> = .54               | M: 14 (1)<br>F: 11 (0) | <i>t</i> (20) = -1.39<br><i>p</i> = .18                   | M: 15 (0)<br>F: 16 (0) | <b><i>t</i>(25) = -3.15</b><br><b><i>p</i> &lt; .01*</b>  |
| <i>RamD-Lt</i> ( <i>p</i> = 0.6068)      | M: 16 (0)<br>F: 10 (0) | <i>t</i> (12) = 0.34<br><i>p</i> = .74  | M: 11 (1)<br>F: 11 (1) | <i>t</i> (17) = 0.00<br><i>p</i> > .99                | M: 14 (2)<br>F: 11 (0) | <i>t</i> (20) = 1.89<br><i>p</i> = .07                    | M: 15 (0)<br>F: 16 (0) | <b><i>t</i>(28) = -3.11</b><br><b><i>p</i> = .004*</b>    |
| <i>MentD</i> ( <i>p</i> = 0.2004)        | M: 16 (0)<br>F: 10 (0) | <i>t</i> (12) = 1.37<br><i>p</i> = .20  | M: 11 (0)<br>F: 11 (0) | <i>t</i> (19) = -1.44<br><i>p</i> = .17               | M: 14 (1)<br>F: 11 (0) | <i>t</i> (20) = 0.36<br><i>p</i> = .72                    | M: 15 (1)<br>F: 16 (0) | <b><i>t</i>(25) = -3.67</b><br><b><i>p</i> = .001*</b>    |
| <i>GonAng-Lt</i> ( <i>p</i> = 0.7782)    | M: 16 (0)<br>F: 10 (0) | <i>t</i> (15) = -0.42<br><i>p</i> = .68 | M: 11 (0)<br>F: 11 (1) | <b><i>t</i>(18) = -2.96</b><br><b><i>p</i> = .01*</b> | M: 14 (1)<br>F: 11 (1) | <i>t</i> (16) = 0.08<br><i>p</i> = .94                    | M: 15 (0)<br>F: 16 (0) | <b><i>t</i>(28) = -4.74</b><br><b><i>p</i> &lt; .001*</b> |
| <i>GnathAng</i> ( <i>p</i> = 0.3647)     | M: 16 (0)<br>F: 10 (0) | <i>t</i> (17) = -0.27<br><i>p</i> = .79 | M: 11 (0)<br>F: 11 (0) | <i>t</i> (14) = -0.49<br><i>p</i> = .63               | M: 14 (1)<br>F: 11 (0) | <b><i>t</i>(19) = -4.41</b><br><b><i>p</i> &lt; .001*</b> | M: 15 (0)<br>F: 16 (0) | <b><i>t</i>(28) = -4.46</b><br><b><i>p</i> &lt; .001*</b> |
| <i>LingAng</i> ( <i>p</i> = 0.5359)      | M: 16 (1)<br>F: 10 (0) | <i>t</i> (21) = -0.96<br><i>p</i> = .35 | M: 11 (0)<br>F: 11 (1) | <i>t</i> (19) = -0.51<br><i>p</i> = .61               | M: 14 (0)<br>F: 11 (0) | <i>t</i> (23) = -1.92<br><i>p</i> = .07                   | M: 15 (0)<br>F: 16 (0) | <i>t</i> (29) = -0.28<br><i>p</i> = .78                   |

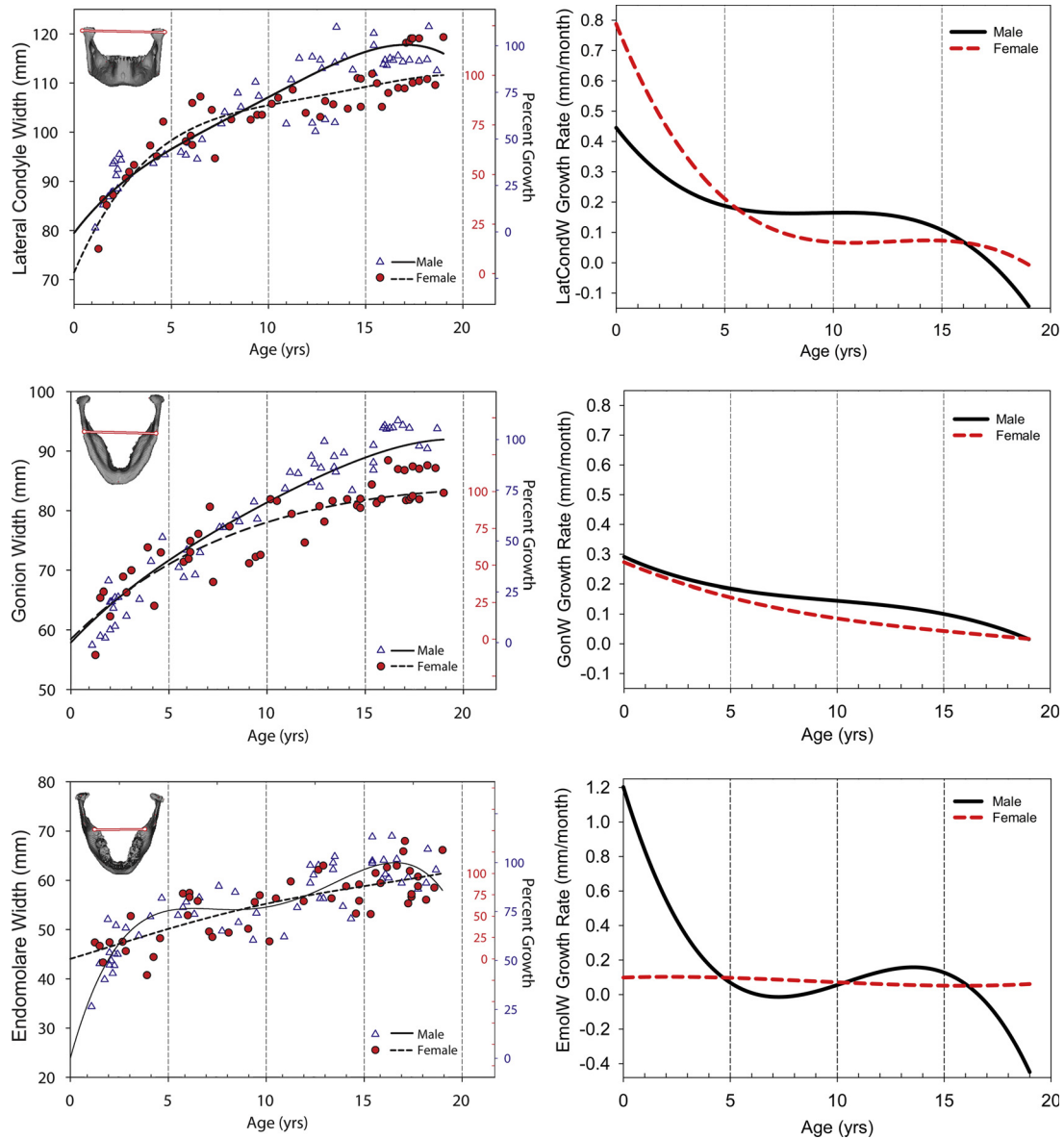


**Fig. 2.** Mandibular width variables *Lateral Condyle Width* (top), *Gonion Width* (center), and *Endomolare Width* (bottom) over the course of development. The left panel shows width measurements in mm from male (open triangle) and female (shaded circle) mandibles as a function of age in years. The data are fitted with growth curve/trend using a fourth degree polynomial fit for male (solid line) and female (dashed line) mandibles. The second y-axis on the right displays the percent growth of adult size for males (outward tick orientation) and females (inward tick orientation). The right panel shows the growth rate as a function of age as derived from its corresponding growth trend fit in the left panel.

As for angular measurements, all three angular variables: gonion angle (*GonAng-Lt*), gnathion angle (*GnathAng*), and lingual angle (*LingAng*) became more acute over time (thus appearing as a negative growth fit) with a tendency for the male mandibles to have more obtuse angular measurements than female mandibles throughout the age range examined (see Fig. 4, left panel). All angular measurements rapidly decreased during the first five years of life, after which changes in mandibular shape, as demonstrated by the angular measurements, gradually decreased. Between eight and ten years, sex differences became more apparent, especially for the gonion and gnathion angles (*GonAng-Lt* and *GnathAng*). At approximately age fifteen, the observed decreases in angular measurements slowed dramatically particularly for the gonion and lingual angles (*GonAng-Lt* and *LingAng*), which are related to the width of the base of the mandible. Similar to the linear variables, the age at which sex differences in growth trend surfaced

(Fig. 4, left panel), was always a few years after changes in growth rate (Fig. 4, right panel).

### 3.2. Growth type: neural and somatic contributions

Mandibular growth followed both the neural and somatic growth types depending on the plane of growth. Percent contributions of each growth type for the nine variables are summarized in Table 4, along with the percent of total growth at age 5, the latter being an important consideration in determining growth type. In general, structures growing in the horizontal plane, with growth predominantly in the anterior-posterior or medial-lateral direction tended to display more of a neural growth type, while structures growing in the vertical plane tended to exhibit more of a somatic growth type. The only exceptions were seen in female mandibles in endomolare width (*EmoIW-Female*), which

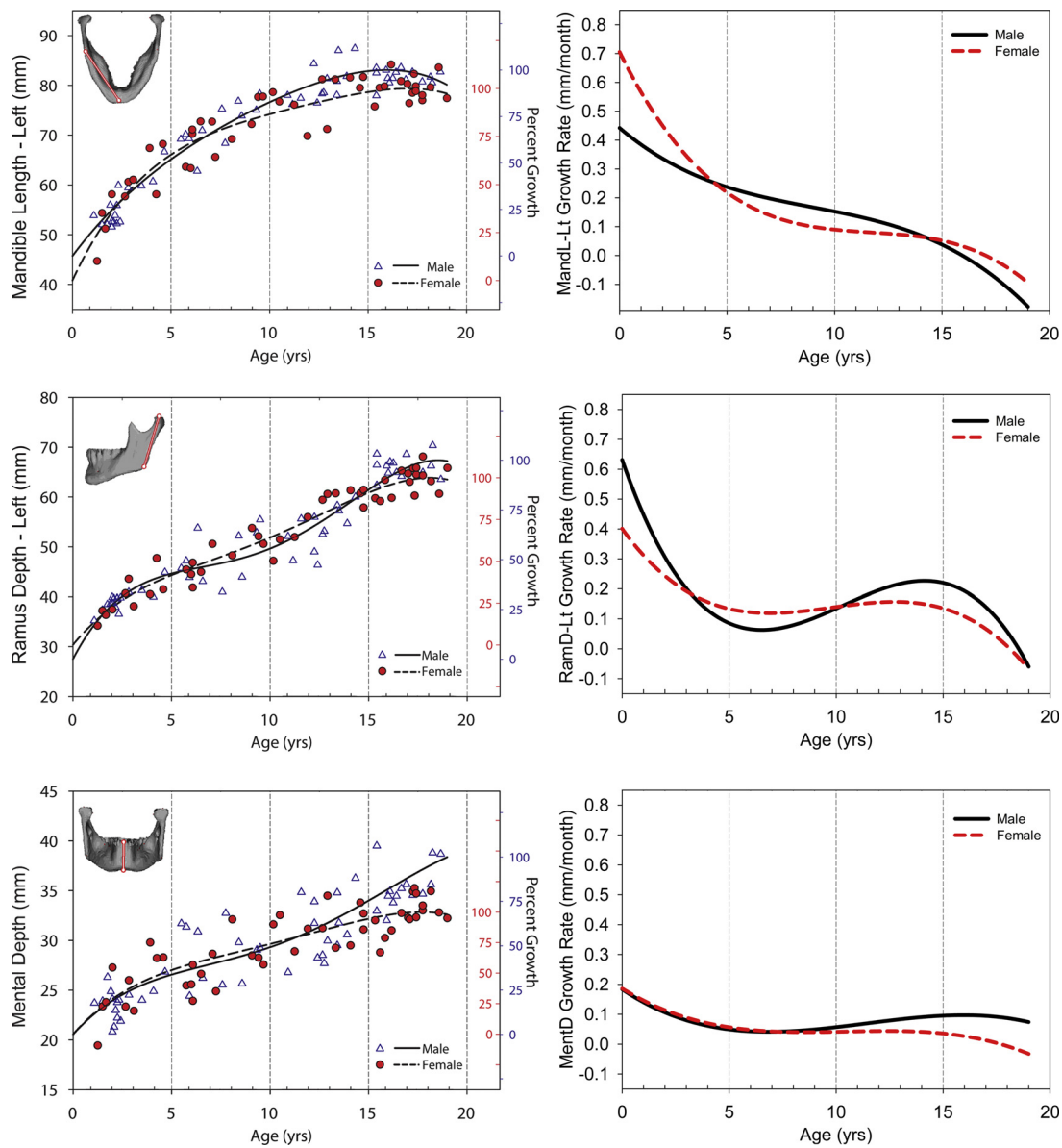


**Fig. 3.** Mandibular length and depth variables *Mandible Length* (top), *Ramus Depth* (center), and *Mental Depth* (bottom) over the course of development. The left panel shows mandibular length and depth measurements in mm from males (open triangle) and females (shaded circle) as a function of age in years. The data are fitted with growth curve/trend using a fourth degree polynomial fit for male (solid line) and female (dashed line) mandibles. The second y-axis on the right displays the percent growth of adult size for males (outward tick orientation) and females (inward tick orientation). The right panel shows the growth rate as a function of age as derived from its corresponding growth trend fit in the left panel.

had a mixed neural and somatic growth trend, and mental depth (*MentD-Female*), which surprisingly displayed a predominantly neural growth. Additionally, a significant positive correlation was found between the neural contribution to growth and percent of adult size reached at age five ( $r(N = 12) = 0.586, p < .05$ ) supporting the expectation that measurements having higher neural contributions to growth were closer to their mature size by age five.

### 3.3. Sexual dimorphism

Three of the nine variables tested for overall sex differences were significant: gonion width (*GonW*,  $p < .001$ ), mandible length (*MandL-Lt*,  $p < .05$ ), and endomolare width (*EmolW*,  $p < .05$ ). The  $p$  values of the likelihood ratio test are listed in Table 3, column 1. However, the findings on endomolare width need to be interpreted with caution given the larger measurement error between raters.

As for localized sex differences in the four age-cohorts for each of the nine variables, findings revealed a total of nine comparisons that reached significance at the .05 Bonferroni-corrected threshold (Bland & Altman, 1995). In general, the older-age cohorts tended to show greater disparities based on sex, with males having greater average linear and angular measurements than females. As listed in Table 3 and displayed in Figs. 5 and 6, six of the significant results occurred in postpubertal cohort IV, the oldest age cohort (*GonW*, *MandL-Lt*, *RamD-Lt*, *MentD*, *GonAng-Lt*, *GnathAng*); two in pubertal cohort III (*GonW*, *GnathAng*); one in prepubertal cohort II (*GonAng-Lt*); and none in prepubertal cohort I, the youngest age cohort. Such localized analysis highlights the variables that show sexual dimorphism during the course of development, and underscores that dimorphism emerges earlier in the inferior aspect of the mandible namely gonion width (*GonW*) and gonion angle, (*GonAng*) than its superior aspect.

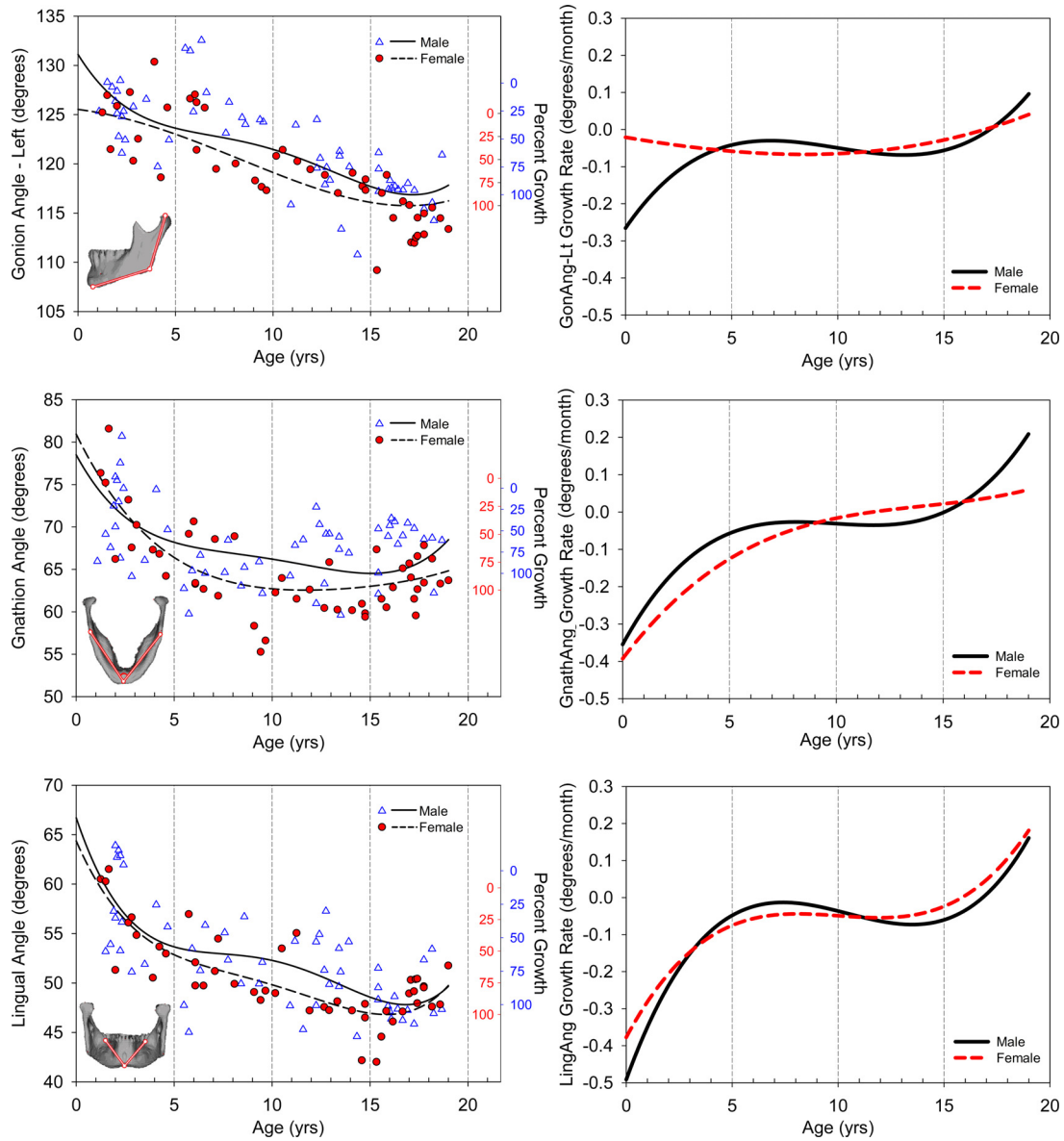


**Fig. 4.** Mandibular angular variables *Gonion angle* (top), *Gnathion Angle* (center), and *Lingual Angle* (bottom) over the course of development. The left panel shows mandibular angular measurements in degrees from male (open triangle) and female (shaded circle) mandibles as a function of age in years. The data are fitted with growth curve/trend using a fourth degree polynomial fit for male (solid line) and female (dashed line) mandibles. The second y-axis on the right displays the percent growth of adult size for males (outward tick orientation) and females (inward tick orientation). The right panel shows the growth rate as a function of age as derived from its corresponding growth trend fit in the left panel.

**Table 4**  
Percent neural versus somatic growth type contribution for each of the six linear variables (column 1) with sex-specific calculations of male and female mandibles. The last column lists percent of mature size at age five, an important factor when examining growth type.

| Variable<br>Abbreviation | Percent contributions to growth: Males |         | Percent contributions to growth: Females |         | Growth by Age 5 |        |
|--------------------------|--|---------|--|---------|-----------------|--------|
|                          | Neural                                 | Somatic | Neural                                   | Somatic | Male            | Female |
| <i>LatCondW</i>          | 100                                    | 0       | 92                                       | 8       | 45%             | 67%    |
| <i>GonW</i>              | 91                                     | 9       | 97                                       | 3       | 41%             | 51%    |
| <i>EmolW</i>             | 94                                     | 6       | 41                                       | 59      | 76%             | 36%    |
| <i>MandL-Lt</i>          | 96                                     | 4       | 99                                       | 1       | 53%             | 66%    |
| <i>RamD-Lt</i>           | 15                                     | 85      | 6  | 94      | 43%             | 42%    |
| <i>MentD</i>             | 28                                     | 72      | 92                                       | 8       | 34%             | 53%    |
| <i>GonAng-Lt</i>         | 14                                     | 86      | 1  | 99      | 53%             | 26%    |
| <i>GnathAng</i>          | 62                                     | 38      | 76                                       | 24      | 74%             | 80%    |
| <i>LingAng</i>           | 56                                     | 44      | 79                                       | 21      | 69%             | 66%    |

Primary contribution to growth.



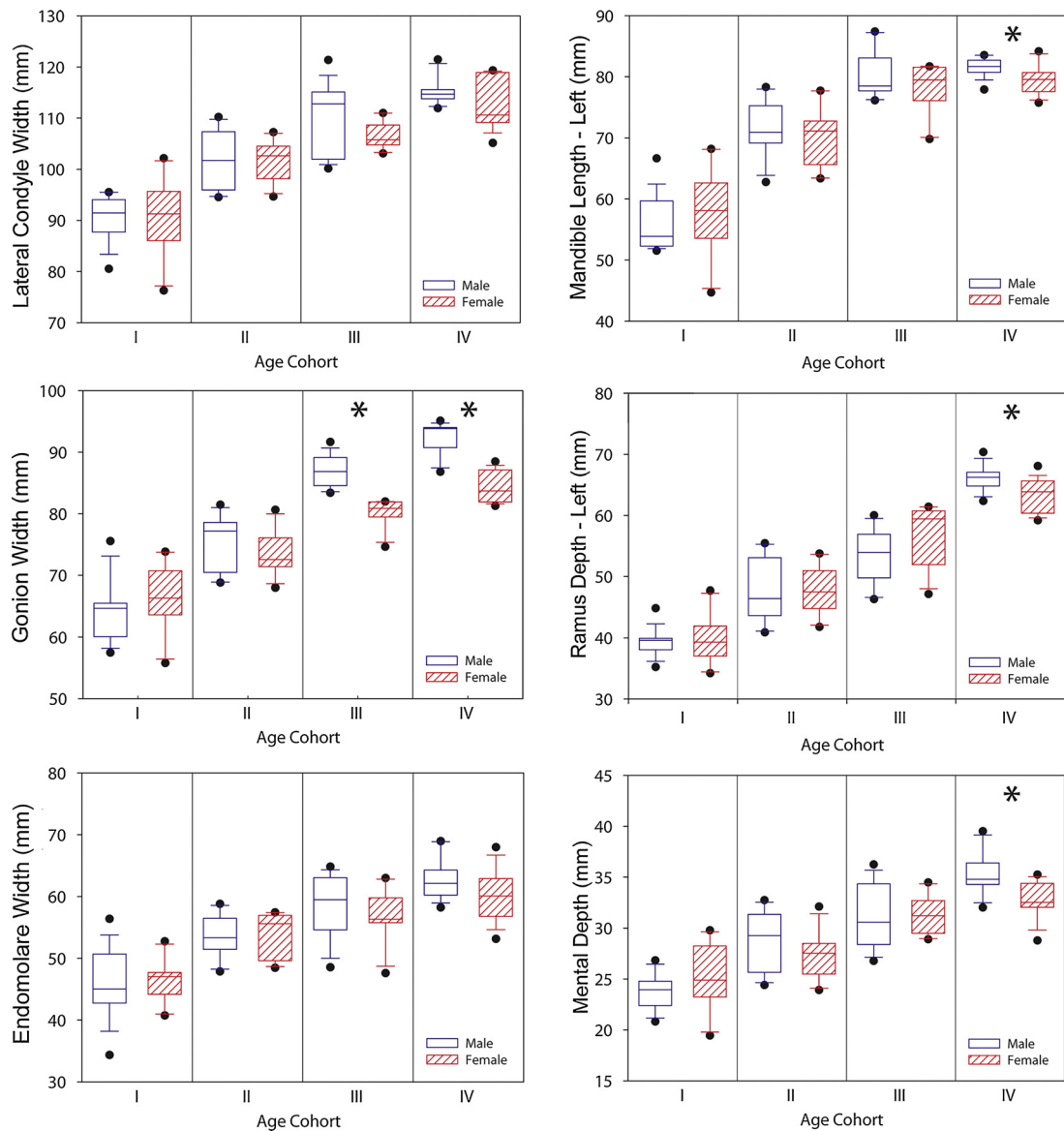


**Fig. 5.** Box plots of linear measurements for mandibular width (left panel), length and depth (right panel) comparing males (open box) versus females (hashed box) at four discrete age cohorts [Cohort I = ages birth –4;11 (years;months); Cohort II = ages 5;00-9;11; Cohort III – ages 10;00-14;11; and Cohort IV = ages 15;00-19;110] for the variables *Lateral Condyle Width* (top left), *Gonion Width* (center left), *Endomolare Width* (bottom left), *Mandible Length* (top right), *Ramus Depth* (center right), and *Mental Depth* (bottom right). The box plots display the 25th to 75th percentile scores and the mean (solid line). The whiskers display the 5th and 95th percentile scores, and outliers are displayed as dots. Significant age cohort sex differences are indicated with an asterisk ( $p < .05$ ). The numeric values for overall sex differences as well as for each age cohort are listed in [Table 3](#).

#### 4. Discussion

The present study quantified the growth of the mandible in three dimensions using a novel approach involving the placement of mandibular landmarks on 3DCT models, from which accurate and reliable linear and angular measurements were derived. The findings of this study provide detailed information on the sex-specific developmental changes of the typically developing mandible during approximately the first two decades of life. The data presented are unique in that they quantify the growth trend, rate, and type for nine variables and identify commonalities in growth based on the plane of structures (horizontal versus vertical). Furthermore, the analysis approach using smaller, developmentally relevant age groups was effective in unveiling prepubertal sexual dimorphism that can be easily masked by differences in growth rate.

Mandibular growth, as expected, was nonlinear. In general, both male and female mandibles displayed rapid growth during the first five years of life, with male mandibles showing an additional pronounced growth spurt during puberty. In general, structures growing in the antero-posterior and medial-lateral dimensions (i.e. the horizontal plane; lateral condyle, gonion and endomolare widths and mandible length), were predominantly neural in type, showing rapid early growth (reaching over 50% of their adult mature size by about age five) and a less pronounced pubertal growth spurt. In contrast, growth in the infero-superior dimension (i.e. the vertical plane; ramus depth) tended to be predominantly somatic in character, displaying less rapid early growth with measurements not exceeding 50% of their adult mature size by age five, and a more pronounced pubertal growth spurt than structures following neural growth trends. Such findings are in line with our hypothesis and our previous work (Vorperian et al., 2009) where

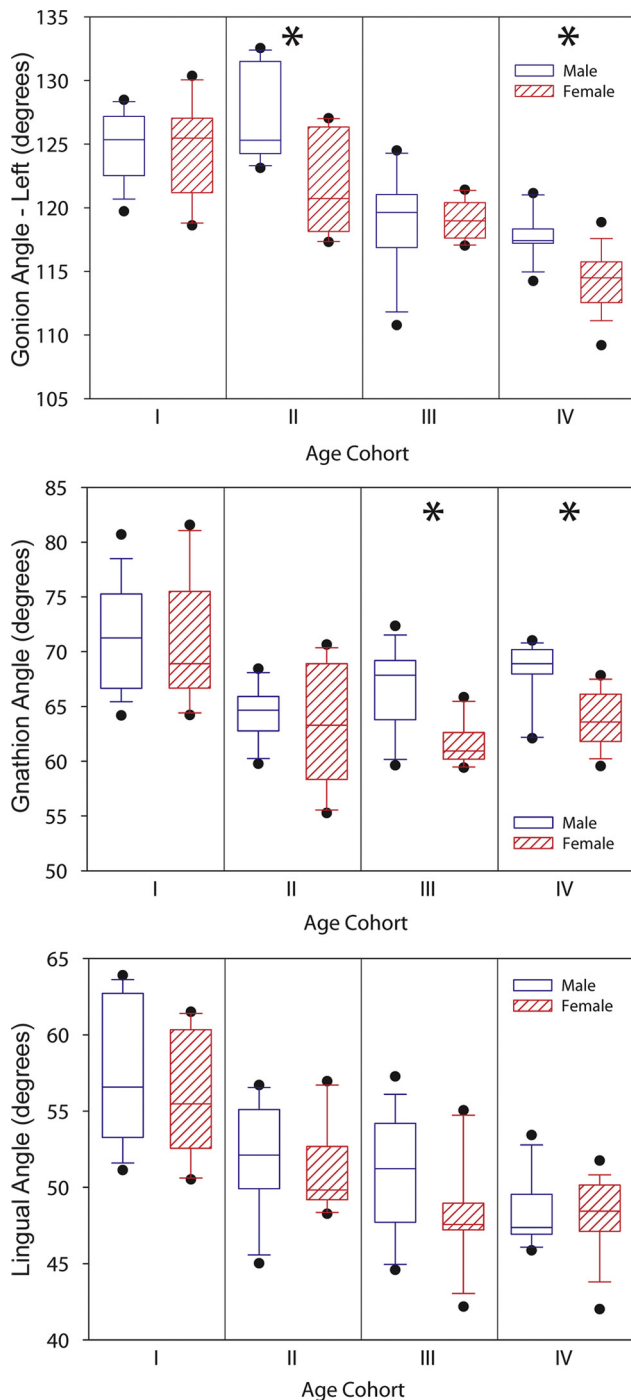


**Fig. 6.** Box plots of angular measurements comparing male (open box) versus female (hatched box) mandibles at four discrete age cohorts (each spanning five years) for the variables *Gonion Angle* (top), *Gnathion Angle* (center) and *Lingual Angle* (bottom panel). The box plots display the 25th to 75th percentile scores and the mean (solid line). The whiskers display the 5th and 95th percentile scores, and outliers are displayed as dots. Significant age cohort sex differences are indicated with an asterisk ( $p < .05$ ). The numeric values for overall sex differences as well as for each age cohort are listed in Table 3.

we found that the oral portion of the vocal tract (in the horizontal plane) exhibited primarily neural growth, whereas the pharyngeal portion of the vocal tract (in the vertical plane) exhibited primarily somatic growth.

Characterization of the non-linear and non-uniform growth of the mandible in terms of neural and somatic growth type contributions (Scammon, 1930; Vorperian et al., 2009) provides

a unique way to characterize the growth of one or more objects along different planes (c.f. Gillgrass & Welbury, n.d.). Comparisons can thus be made within a structure and related to measurements across craniofacial structures (e.g., medial-lateral growth of the mandible and the hyoid bone). Such an assessment may also be applied to other structures, particularly structures whose growth may be a true mixture of different growth types (Gillgrass & Welbury, n.d.; Vorperian et al., 2009)

Several variables, specifically mandible length (Fig. 3, top panel), ramus depth (Fig. 3, center panel) and the angular measure between those two distance measurements, gonion angle (Fig. 4, top panel), displayed downward and forward growth of the mandible throughout childhood. We observed primarily anterior-posterior growth of the mandible during the first five years of life, with mandibular length exhibiting more growth than ramus depth. During puberty, mandible growth was primarily downward with ramus depth exhibiting more growth than mandibular length. Our findings expand upon the work of Martinez-Maza et al. (2013) who compared bone remodeling in subadult/pediatric mandibles and adult mandibles. They observed a primarily downward growth pattern in subadult specimens, but since children were combined into a single subadult group, growth differences between early childhood and puberty were not examined.

As for sex differences, our data show that, in line with the noted craniofacial sex differences at birth (Nellhaus, 1968), there are size and shape differences in male and female mandibles early on in life. However, such differences are not necessarily unidirectional as some variables are slightly larger in females than males. Our data also confirm the findings of Coquerelle et al. (2011) that sex differences in size and shape change during the course of development, particularly during the first ten years of life (cohorts I and II), as shown in the left panel of Figs. 2–4. At about age eight to ten years of age, growth in males begins to outpace that of females and gives rise to apparent trends in sexual dimorphism a few years later, typically between ten and fifteen years of age (cohort III). In general, by age 15 the male mandibles have larger linear and angular measurements than female mandibles with the measurements of gonion width and mandible length being significantly larger in the male mandibles.

Localized assessment of sexual dimorphism based on the four age cohorts revealed that significant sex difference emerged as early as prepubertal cohort II (ages 5.00 to 9.11 years) for the gonion angle. However, such differences dissipated during pubertal cohort III (ages 10.0 to 14.11 years) – likely due to differences in growth rate – then re-emerged during postpubertal cohort IV (ages 15.00 to 19.11 years). Two additional measurements, gonion width and gnathion angle, showed significant sexual dimorphism during pubertal age cohort III. Such findings further highlight that dimorphism in the anterior-posterior and medial-lateral planes is more apparent on the inferior portion of the mandible (mandible length, gonion width) than the superior portion of the mandible. Gnathion angle, a measure of chin protrusion, is considered to be an important determinant of shape dimorphism and used to determine sex in the forensic sciences (Kano et al., 2015).

A significant secondary growth spurt was revealed during pubertal and postpubertal age cohorts III and IV for mental and ramus depth, particularly in male mandibles, contributing to the distinct differences in size and shape between male and female mandibles. Such growth is in line with studies on craniofacial growth, where the 4- to 5-year-long growth spurt during puberty tends to slow or cease around age 12–15 years for females and 15–17 years in males (Bulygina et al., 2006; Martinez-Maza et al., 2013; Nellhaus, 1968).

The use of three-dimensional landmarks on 3DCT mandible models provides a highly accurate approach to quantifying typical

mandibular growth. This methodological improvement helps overcome a number of problems associated with measurements derived from medical imaging studies, such as patient position and the use of a single 'slice' of data to characterize the growth of complex structures such as the mandible. Previously, midsagittal images of the mandible have been used to compare mandibular shape and size; however, such analyses omit the medial-lateral dimension, which has important implications related to airway caliber and neurocranium size. Furthermore, the use of three-dimensional landmarks provides a simple way to make accurate measurements within and across craniofacial structures, such as the hyoid or the skull base, providing information on the relational growth of functionally related structures (e.g., descent of the hyoid bone relative to the mandible). The application of similar methodologies, including the characterization of growth trend, growth type and sex-based comparisons at developmentally important ages would help assess the growth trends of structurally and/or functionally related structures.

Population-based growth charts provided by the CDC and the World Health Organization (WHO) (Kuczumarski et al., 2002) and the Anthropometric Reference (Fryar et al., 2012) provide a normative metric against which atypical growth can be compared to aid in disease treatment and assessment of treatment outcomes. While the Anthropometric Reference (Fryar et al., 2012) offers sex-specific normative data on several anatomic structures it provides no data on the mandible. The Bolton Standard (Broadbent et al., 1975) is the commonly used reference providing detailed radiographic data from 16 boys and 16 girls ages 1 to 18 years. However, like the Anthropometric Reference (Fryar et al., 2012), it does not offer a detailed assessment of general growth trends. By quantifying sex-specific mandibular growth in multiple planes and identifying differences in the growth trend, rate, and type (e.g., neural/somatic) of various mandibular measurements, the data gathered in this study can serve as a normative reference on the growth pattern of the mandible for the assessment of atypical mandibular growth can be assessed such as the micrognathia common among individuals with Down syndrome.

While the sample used in this study was sufficiently large to conduct the necessary analyses, a larger sample would provide more detailed normative data. Additionally, more specific age-based comparisons of sex differences, as used in Vorperian et al. (2011), would become feasible, providing even more specific information on the temporal development of sex differences in mandibular dimensions. Furthermore, while the fourth degree mixed-effect polynomial fit and its derivative provided a good overview of developmental trend and growth rate, insufficient data and/or data variability at the extreme age range examined can exacerbate the limitation of this approach, where some measurements (e.g., endomolare width in males) briefly displayed negative growth rates at the lower and upper ends of the age range. The application of a composite growth model, as outlined by Wang et al. (2016), will likely overcome this limitation of the fourth-degree mixed-effect polynomial fit. Additionally, rendering developmental 3DCT mandible models can be used to quantify surface area growth in all planes (Chung, Qiu, Seo, & Vorperian, 2015).

Growth of the craniofacial complex can be affected by the structural and functional relationships between its component parts. These relationships can be elucidated by quantifying and examining typical and atypical growth (e.g., cases where mandibular function is compromised). For example, our findings show that lateral condyle width exhibits a strong neural growth trend, as would be expected due to its structural articulation with the cranium. Functional use of structures plays an important role in growth patterns (Carlson, 2005) and interruptions or abnormalities in mandibular function result in abnormalities in mandibular form (Moss & Rankow, 1968; Moss, 1997). For example, infants

with Down syndrome experience feeding and sucking difficulties (Bull et al., 2011; Spender et al., 1996), which may affect mandibular growth. Additional studies might include the effect of bite force on ramus depth growth when toddlers' chewing evolves from a munching pattern into a rotary chewing pattern as molars emerge (Wilson & Green, 2009).

While the specific mechanisms driving mandibular growth are beyond the scope of the present study, the data provided by analysis of mandible growth in three dimensions provides preliminary normative data for clinical assessment and study of craniofacial growth. This normative representation of mandibular growth can be used to guide future analyses, including comparisons of mandibular growth between different populations and the analysis of the interaction between mandibular structure and function.

In conclusion, this study quantified six linear and three angular measurements of the typically developing mandible in males and females during approximately the first two decades of life. Findings reveal that structures in the horizontal plane such as condylar width and mandibular body length generally mature sooner than structures in the vertical plane such as ramus depth. Differences in growth rate between males and females obscure prepubertal sexual dimorphism particularly since the direction of dimensional differences is not the same across the different variables. Using smaller age-group comparisons across the two sexes helped reveal sex-differences in the inferior aspect of the mandible between the ages of five and ten. The data presented here can be used as a normative reference by multiple disciplines including dentistry, facial surgery, and forensics.

#### Conflict of interests

None.

#### Acknowledgements

Funding: This work was supported, in part, by National Institutes of Health (NIH) Grants R01 DC006282 from the National Institute on Deafness and Other Communicative Disorders (NIDCD), and Core Grant P-30 HD0335 and U54 HD090256 from the National Institute of Child Health and Human Development (NICHD). The funding sources had no involvement in study design, data collection, analysis, interpretation, writing of this paper, or its submission for publication.

We thank Meghan M Cotter, Brian J. Whyms, Eugene M. Schimek, and Reid Durtschi for assistance with 3DCT modeling and landmarking efforts; we also thank Ying Ji Chuang for assistance with reliability measure calculations, and Erin M. Wilson, Ray D. Kent, and Jacqueline Houtman for comments on earlier versions of this manuscript.

#### References

- Björk, A. (1969). Prediction of mandibular growth rotation. *American Journal of Orthodontics*, 55(6), 585–599.
- Bland, J. M., & Altman, D. G. (1995). Multiple significance tests: The Bonferroni method. *BMJ*, 310(6973), 170.
- Broadbent, B. H. Sr., Broadbent, B. H. Jr., & Golden, W. H. (1975). *Bolton standards of dentofacial developmental growth*. CV Mosby.
- Bull, M. J., Capone, G. T., Cooley, W. C., Mattheis, P., Robison, R. J., Saul, R. A., . . . Spire, P. (2011). Clinical Report—Health supervision for children with down syndrome. *Pediatrics*, 128(2), 393–406. <http://dx.doi.org/10.1542/peds.2011-1605>.
- Bulygina, E., Mitteroecker, P., & Aiello, L. (2006). Ontogeny of facial dimorphism and patterns of individual development within one human population. *American Journal of Physical Anthropology*, 131(3), 432–443. <http://dx.doi.org/10.1016/j.amj.2015.02.003>.
- Carlson, D. S. (2005). Theories of craniofacial growth in the postgenomic era. *Seminars in Orthodontics*, 11(4), 172–183. <http://dx.doi.org/10.1053/j.sodo.2005.07.002>.

- Chung, D., Chung, M. K., Durtschi, R. B., & Vorperian, H. K. (2008). Determining length-based measurement consistency from magnetic resonance images. *Academic Radiology*, 15, 1322–1330. <http://dx.doi.org/10.1016/j.acra.2008.04.020>.
- Chung, M. K., Qiu, A., Seo, S., & Vorperian, H. K. (2015). Unified heat kernel regression for diffusion kernel smoothing and wavelets on manifolds and its application to mandible growth modeling in CT images. *Medical Image Analysis*, 22(1), 63–76. <http://dx.doi.org/10.1016/j.media.2015.02.003>.
- Coquerelle, M., Bookstein, F. L., Braga, J., Halazonetis, D. J., Weber, G. W., & Mitteroecker, P. (2011). Sexual dimorphism of the human mandible and its association with dental development. *American Journal of Physical Anthropology*, 145(2), 192–202. <http://dx.doi.org/10.1002/ajpa.21485>.
- Enlow, D. H., & Hans, M. G. (Eds.). (1996). *Essentials of facial growth*. WB Saunders Company.
- Enlow, D. H., & Harris, D. B. (1964). A study of the postnatal growth of the human mandible. *American Journal of Orthodontics*, 50(1), 25–50.
- Fitch, W. T., & Giedd, J. (1999). Morphology and development of the human vocal tract: A study using magnetic resonance imaging. *The Journal of the Acoustical Society of America*, 106, 1511–1522.
- Franklin, D., Oxnard, C. E., O'Higgins, P., & Dadour, I. (2007). Sexual dimorphism in the subadult mandible: Quantification using geometric morphometrics. *Journal of Forensic Sciences*, 52(1), 6–10. <http://dx.doi.org/10.1111/j.1556-4029.2006.00311.x>.
- Fryar, C. D., Gu, Q., Ogden, C. L. (2012). Anthropometric reference data for children and adults: United States, 2007–2010. *Vital and health statistics. Series 11, Data from the national health survey* (252), 1–48.
- Gillgrass, T. J., Welbury, R. (n.d.). Craniofacial growth and occlusal development. In *Orthodontics I: development, assessment, and treatment planning*. (9.1) Retrieved from <http://pocketdentistry.com/9-orthodontics-i-development-assessment-and-treatment-planning/>.
- Humphrey, L. T. (1998). Growth patterns in the modern human skeleton. *American Journal of Physical Anthropology*, 105(1), 57–72.
- Jacob, H. B., & Buschang, P. H. (2014). Mandibular growth comparisons of Class I and Class II division 1 skeletofacial patterns. *The Angle Orthodontist*, 84(5), 755–761. <http://dx.doi.org/10.2319/100113-719.1>.
- Kano, T., Oritani, S., Michiue, T., Ishikawa, T., Hishmat, A. M., Sogawa, N., . . . Maeda, H. (2015). Postmortem CT morphometry with a proposal of novel parameters for sex discrimination of the mandible using Japanese adult data. *Legal Medicine*, 17(3), 167–171. <http://dx.doi.org/10.1016/j.legalmed.2014.12.009>.
- Krarup, S., Darvann, T. A., Larsen, P., Marsh, J. L., & Kreiborg, S. (2005). Three-dimensional analysis of mandibular growth and tooth eruption. *Journal of Anatomy*, 207(5), 669–682. <http://dx.doi.org/10.1111/j.1469-7580.2005.00479.x>.
- Kuczmariski, R. J., Ogden, C. L., Guo, S. S., Grummer-Strawn, L. M., Flegal, K. M., Mei, Z., & Johnson, C. L. (2002). 2000 CDC Growth Charts for the United States: methods and development. *Vital and health statistics. Series 11, Data from the national health survey*, (246), 1–190.
- Martinez-Maza, C., Rosas, A., & Nieto-Díaz, M. (2013). Postnatal changes in the growth dynamics of the human face revealed from bone modelling patterns. *Journal of Anatomy*, 223(3), 228–241. <http://dx.doi.org/10.1111/joa.12075>.
- Moss, M. L., & Rankow, R. M. (1968). The role of the functional matrix in mandibular growth. *The Angle Orthodontist*, 38(2), 95–103.
- Moss, M. L. (1997). The functional matrix hypothesis revisited. 4. The epigenetic antithesis and the resolving synthesis. *American Journal of Orthodontics and Dentofacial Orthopedics*, 112(4), 410–417.
- Nellhaus, G. (1968). Head circumference from birth to eighteen years practical composite international and interracial graphs. *Pediatrics*, 41(1), 106–114.
- Rosas, A., & Bastir, M. (2002). Thin-plate spline analysis of allometry and sexual dimorphism in the human craniofacial complex. *American Journal of Physical Anthropology*, 117(3), 236–245. <http://dx.doi.org/10.1002/ajpa.10023>.
- Scammon, R. E. (1930). The measurement of the body in childhood. In J. A. Harris, C. M. Jackson, D. G. Paterson, & R. E. Scammon (Eds.), *The measurement of man* (pp. 173–215). Minneapolis, MN: University of Minnesota Press.
- Smartt, J. E., Low, D. W., & Bartlett, S. P. (2005a). The pediatric mandible: I. A primer on growth and development. *Plastic and Reconstructive Surgery*, 116(1), 14e–23e. <http://dx.doi.org/10.1097/01.PRS.0000169940.69315.9C>.
- Smartt, J. E., Low, D. W., & Bartlett, S. P. (2005b). The pediatric mandible: II. Management of traumatic injury or fracture. *Plastic and Reconstructive Surgery*, 116(1). <http://dx.doi.org/10.1097/01.prs.0000173445.10908.f8>.
- Spender, Q., Stein, A., Dennis, J., Reilly, S., Percy, E., & Cave, D. (1996). An exploration of feeding difficulties in children with Down syndrome? *Developmental Medicine and Child Neurology*, 38(8), 681–694.
- Tanner, J. M. (1962). *Growth at adolescence*, 2nd ed. Oxford, United Kingdom: Blackwell Scientific.
- Vorperian, H. K., Wang, S., Chung, M. K., Schimek, E. M., Durtschi, R. B., Kent, R. D., & Gentry, L. R. (2009). Anatomic development of the oral and pharyngeal portions of the vocal tract: An imaging study. *The Journal of the Acoustical Society of America*, 125(3), 1666–1678. <http://dx.doi.org/10.1121/1.3075589>.
- Vorperian, H. K., Wang, S., Schimek, E. M., Durtschi, R. B., Kent, R. D., Gentry, L. R., & Chung, M. K. (2011). Developmental sexual dimorphism of the oral and pharyngeal portions of the vocal tract: An imaging study. *Journal of Speech, Language, and Hearing Research*, 54(4), 995–1010. [http://dx.doi.org/10.1044/1092-4388\(2010\)10-0097](http://dx.doi.org/10.1044/1092-4388(2010)10-0097).
- Walker, G. F., & Kowalski, C. J. (1972). On the growth of the mandible. *American Journal of Physical Anthropology*, 36, 111–118.
- Wang, Y., Chung, M. K., & Vorperian, H. K. (2016). Composite growth model applied to human oral and pharyngeal structures and identifying the contribution of growth types. *Statistical Methods in Medical Research*, 25, 1975–1990. <http://dx.doi.org/10.1177/0962280213508849>.
- Whyms, B. J., Vorperian, H. K., Gentry, L. R., Schimek, E. M., Bersu, E. T., & Chung, M. K. (2013). The effect of computed tomographic scanner parameters and 3-dimensional volume rendering techniques on the accuracy of linear, angular, and volumetric measurements of the mandible. *Oral Surgery, Oral Medicine, Oral Pathology and Oral Radiology*, 115(5), 682–691. <http://dx.doi.org/10.1016/j.oooo.2013.02.008>.
- Wilson, E. M., & Green, J. R. (2009). The development of jaw motion for mastication. *Early Human Development*, 85(5), 303–311. <http://dx.doi.org/10.1016/j.earlhumdev.2008.12.003>.